Complex Brain–Heart Mapping in Mental and Physical Stress

VINCENZO CATRAMBONE^{ID}, (Member, IEEE), AND GAETANO VALENZA^{ID}, (Senior Member, IEEE)

Neurocardiovascular Intelligence Laboratory, Bioengineering and Robotics Research Center E. Piaggio, and Department of Information Engineering,
School of Engineering, University of Pisa, 56126 Pisa, Italy

CORRESPONDING AUTHOR: V. CATRAMBONE (vincenzo.catrambone@ing.unipi.it)

ABSTRACT Objective: The central and autonomic nervous systems are deemed complex dynamic systems, wherein each system as a whole shows features that the individual system sub-components do not. They also continuously interact to maintain body homeostasis and appropriate react to endogenous and exogenous stimuli. Such interactions are comprehensively referred to functional brain–heart interplay (BHI). Nevertheless, it remains uncertain whether this interaction also exhibits complex characteristics, that is, whether the dynamics of the entire nervous system inherently demonstrate complex behavior, or if such complexity is solely a trait of the central and autonomic systems. Here, we performed complexity mapping of the BHI dynamics under mental and physical stress conditions. Methods and procedures: Electroencephalographic and heart rate variability series were obtained from 56 healthy individuals performing mental arithmetic or cold-pressure tasks, and physiological series were properly combined to derive directional BHI series, whose complexity was quantified through fuzzy entropy. Results: The experimental results showed that BHI complexity is mainly modulated in the efferent functional direction from the brain to the heart, and mainly targets vagal oscillations during mental stress and sympathovagal oscillations during physical stress.
Conclusion: We conclude that the complexity of BHI mapping may provide insightful information on the dynamics of both central and autonomic activity, as well as on their continuous interaction. Clinical impact: This research enhances our comprehension of the reciprocal interactions between central and autonomic systems, potentially paving the way for more accurate diagnoses and targeted treatments of cardiovascular, neurological, and psychiatric disorders.

INDEX TERMS Brain–heart interplay, complexity, EEG, heart rate variability, fuzzy entropy.

I. INTRODUCTION

Brain-heart interplay (BHI) refers to the continuous functional communication that affects the activity of the autonomous nervous system (ANS) and the central nervous system (CNS). Studies on BHI can reveal perspectives facilitating the understanding of several patho-physiological conditions [1], [2], [3], [4]. The BHI represents the functional outcome of a network of chemical, electrical, and anatomical connections that link the CNS and ANS, and has been found to originate in the central autonomic network (CAN) [1], [4], [5], [6], [7], [8]. The CAN is not ascribable to a specific brain region, since it encompasses the medullary areas, midbrain, and amygdala, as well as peripheral autonomic terminations and cortical regions (e.g. medial prefrontal cortex, insula) [9], [10]. More specifically, the CAN encompasses several forebrain and brainstem areas as well as the medial prefrontal, insular, and cingulate cortices, extending to the periaqueductal gray matter, hypothalamus, amygdala, and other regions of the medulla (e.g. nucleus of the tractus solitarius, nucleus ambiguous, and others) [7], [11]. CAN areas have specific functions and together perform the complex activity of autonomic regulation; for example, high forebrain areas and the amygdala play primary roles in homeostatic-interoceptive regulation [1], [7], [11].

Physiological variations in functional BHI also occur in relation to several external stimuli, including emotional elicitation [12], sleep stages [13], cognitive load [14], deep breathing [15], and other autonomic manoeuvres [16]. Moreover, BHI time series have been shown to be altered by neuropathological conditions such as mild depression [10], epilepsy [17], and schizophrenia [18].

In this context, the directionality of the phenomenon assumes extreme importance, because most of the attention has been directed toward the neural control of autonomic functions, disregarding the control in the opposite direction and the influence of ANS over CNS activity. Indeed, neural interference on cardiovascular activity has been evaluated in relation to sympathovagal stimuli [16] or mood disorders [10], as well as in the cardiac initiation of electroencephalographic responses in emotional [12] or somatosensory [19] elicitation.

The estimation of functional BHI is associated with a number of technical challenges regarding the methodological approach to be exploited, since it involves multimodal (in most cases EEG and HRV) and multivariate (EEG channels) variables, directionality (the brain–to–heart interplay does not correspond to the heart–to–brain interplay), nonlinearity, and different dynamical features. Several methodologies have been developed for this purpose, and they singularly differ in the main issue addressed: [20], [21], [22] focus on the directionality of the BHI phenomenon, [23], [24] disentanglement between linear and nonlinear interactions; if on one side heartbeat evoked potentials [19] are specific for brain response to the cardiac cycle, other works [16] focus on instantaneous heartbeat response to brain activity; moreover, an ad–hoc synthetic data-generation (SDG) model has been developed and exploited in different contexts considering the peculiarities of the BHI phenomenon [10], [12].

Functional BHI is intrinsically a time-varying phenomenon, because it changes with its own dynamics in response to different stimuli [1]. Brain and cardiovascular time series are widely acknowledged to show highly nonlinear and complex dynamics [25], [26], [27], [28], [29], and BHI is known to extend to the multifractal domain [30]. In this context, it is still unknown whether the time series associated with BHI dynamics shows complex behaviour as well, and if it is modulated by different conditions. In other words, the nervous system as a whole has not been characterised, accounting for its complex and nonlinear nature. Here, we adopt the term complexity to refer to the degree of regularity or predictability of the temporal patterns observed in the signals of interest. Specifically, complexity refers to the unpredictability of the present state of a physiological system, identified by its time series, given a limited number of its past samples [31].

The information-theory-based approaches are commonly employed to quantify short-term complexity. In the frame of time series analysis, these approaches originate from the concept of conditional entropy, which is a measure of the average remaining uncertainty or randomness in a time series,

taking into account its past values [31], [32]. To this extent, conditional entropy-like metrics like approximate entropy, sample entropy, and fuzzy entropy have been proposed to quantify the complexity, irregularity, or unpredictability of time series. However, they differ in their approaches and sensitivity to the intricacies of the data.

Approximate entropy, introduced by Pincus [33], evaluates the regularity or unpredictability of a time series by comparing the likelihood of similar patterns of length m repeating within a certain tolerance level r. While it has been widely used to analyze the complexity of physiological signals, it is sensitive to the choice of parameters m and r, and its value may depend on the length of the time series. Sample entropy [34] was introduced as a refinement of approximate entropy by eliminating self-matches and providing a more consistent estimation of the complexity of a time series. Like approximate entropy, sample entropy compares the occurrence of similar patterns within a tolerance level r, but it is less sensitive to the choice of parameters and the length of the time series. Fuzzy entropy (FuzzyEn) [35], [36] extends the concept of entropy to incorporate the inherent fuzziness or imprecision in real-world data. FuzzyEn employs fuzzy membership functions to quantify the uncertainty and vagueness associated with complex systems more effectively than other entropy measures. It is particularly advantageous when dealing with noisy or imprecise data and provides a more robust and nuanced understanding of the intricacies of real-world time series. FuzzyEn also provides advantages related to low dependency on data length [37].

These advantages come at the cost of defining and tuning an extra parameter, the gradient of the fuzzy membership function boundary, that is to be added to the usual parameter set comprehending similarity tolerance, embedding dimension, and time series length. FuzzyEn has already been exploited in physiological signal processing, specifically in EEG and HRV analysis in different experimental paradigms [38], [39], to investigate brain activity complexity in patients with Alzheimer's disease [38], or cardiovascular activity complexity differences between heart failure patients and healthy controls [39].

In the present study, we performed a FuzzyEn analysis on the BHI series to identify the complex brain-heart mapping in physical and mental stress conditions. To explore the temporal complexity of BHI, we exploited the output of the SDG model [40], which provides time–resolved directional BHI estimates at several frequency bands and scalp locations, applied to two different datasets. The first is associated with cognitive workload performed through consecutive mental arithmetic calculations, and the second is associated with the cold pressor test (CPT), an autonomic maneuver that causes strong sympathovagal elicitation through thermal stress.

More specifically, through CNS manipulation, experimental mental arithmetic approaches can activate the sympathetic nervous system. Participants are usually required to complete various cognitive tasks, often by clicking a button or

performing algebraic calculations in a certain amount of time [41]. Although mental arithmetic tasks have frequently been investigated at the CNS [42], [43] and ANS [44] levels, only a few studies have focused on their functional BHI correlates [22]. In response to stress, variations in cardiac output correlate with neural activity in the left temporal and lateral frontal lobes [45], [46]. Additionally, the BHI appears to grow in size, and the information flow from the scalp's post-central and central regions to the heart appears to grow during mental arithmetic [47].

Several studies, also by the present authors, have extensively investigated the BHI changes during CPT elicitation [16], [30], [48]. The CPT is a test for examining the body's autonomic functioning as well as the CNS response to intense temperature and sub–threshold pain stimuli [49], [50], [51]. Through the enhanced sympathetic activity of the ANS, CPT activates physiological systems such as the baroreflex to maintain the body in a homeostatic state [52]. Pragmatically, it typically entails submerging a distal limb (hand or foot) for a duration between 1 and $5min$ in cold water. Numerous cortical and subcortical brain regions are involved in the brain correlates of CPT, such as frontal regions in various frequency bands, posterior-parietal areas in the alpha band, and peripheral bilateral temporal regions in the beta band [16], [51], [53].

To summarise, this study evaluated two hypotheses: BHI has complex dynamics, and BHI complexity is modulated by physiological changes obtained under different experimental conditions.

II. EXPERIMENTAL DATA AND SIGNAL PREPROCESSING

This section provides a description of the experimental procedure for data gathering. This study received formal approval from the qualified ethics committee of the University of Pisa under protocol number 0036590/2021.

A. MENTAL ARITHMETIC

The first dataset used in our study was the EEG during mental arithmetic tasks dataset [54], which is publicly available and has already been preprocessed. We obtained it from the *Physionet.org* data repository (*https://physionet.org/content/eegmat/1.0.0/*) [55]. This dataset consists of concurrent recordings of electrophysiological brain (EEG) activity, using a 10-20 standard 19 electrodes cap, and a 1-lead cardiovascular (ECG) activity, sampled at a frequency of $500Hz$. The recordings were obtained from 36 healthy volunteers who underwent a $180s$ resting phase and a $60s$ mental cognitive workload task, i.e., performing mental arithmetic (MA).

Recordings from four volunteers were rejected owing to gross artefacts on visual inspection; eventually, data from 32 participants (24 females) were retained for further processing; their average age was of 18 ± 2.01 years. The eligibility criteria were normal or corrected-to-normal visual acuity, normal colour vision, no clinical manifestations of mental or

cognitive impairment, and no learning disabilities. The use of psychoactive medication, drug or alcohol addiction, and psychiatric or neurological complaints were also considered as exclusion criteria.

To preprocess the EEG series, a power line notch filter at $50Hz$ and a $[0.5\ Hz - 45Hz]$ bandpass filter were applied before independent component analysis, which was used to identify artifacts (such as those caused by eyes, muscles, and cardiac pulsation) that were subsequently rejected. Finally, the channel series were re-referenced to the common average, which is the most appropriate method for BHI studies [56]. Further details of signal acquisition and preprocessing can be found in a previous study [54].

As reported in that study [54], volunteers were expected to perform arithmetic tasks consisting of multiple mental subtractions. Based on the number of arithmetic operations completed per minute and the corresponding ease of completing the task, the cohort was divided into two groups. For one group of participants (group *BC*), the task was particularly difficult, whereas for the second group, the task was not particularly challenging (group *GC*). After preprocessing, 10 participants were included in the *BC* group, with a mean number of operations of 7 ± 3.6, while 22 participants were included in the *GC* group, with a mean number of subtractions of 21 ± 7.4.

B. COLD PRESSOR TEST

The second dataset was collected from 30 healthy right-handed individuals (26.7 years on average; 15 males) who volunteered to participate in the study. The participants were seated on a comfortable chair and underwent an initial $3min$ resting state followed by the actual cold pressor stimulation, which consisted of submerging their non–dominant (left) hand into cold water, maintained at approximately $4\,°C$. Participants were asked to hold the position for up to $3min$, which was considered as the time threshold for not eliciting pain perception [50] however, they were free to remove their hand if they felt uncomfortable. For this reason, six participants did not reach $2min$ of cold pressor stimulation, and their data were discarded from further analysis. Physiological signals were recorded using a 128-electrode EEG and a 1-lead ECG obtained with a sampling frequency of $500\,Hz$. Researchers may obtain raw data through reasonable mail requests if ethical requirements are met. After the CPT phase, participants were required to maintain a resting position for another $3min$, thus undergoing a recovery phase.

On one side, an R-beat detection from the ECG series was applied using the well-known Pan–Tompkins algorithm [57], which was followed by an automated and visually inspected artefact rejection, all implemented in Kubios Software [58].

On the other side, EEG signals were preprocessed through the HAPPE pipeline, which has been extensively described elsewhere [59] and implemented through the EEGLAB toolbox in MatLab software (MathWorks Inc.) [60]. Briefly, 38 more external channels were rejected, and a bandpass

filter between 1 Hz and 100 Hz and a notch filter at 50 Hz were applied. Subsequently, bad channels were removed after identification as the most external 1% tail of a joint distribution based on high-order statistical moments. The HAPPE pipeline implements a wavelet-enhanced independent component analysis to detect and remove periodic artifacts (e.g. eye blinks, heartbeats, respiration), followed by an automated ICA-based algorithm to remove the remaining artifacts (e.g. muscular and motor) [59]. Eventually, the electrodes removed as external joint distribution tails were spherically interpolated, and the final 90 channels were re-referenced to the common average as the most appropriate method for BHI studies [56].

C. SIGNAL PROCESSING

The time-resolved power spectral density (PSD) of the EEG series was calculated using a short-time Fourier transform, employing a 1000 samples Hamming window (equivalent to 2 seconds) and a 0.5 second step, yielding a $2Hz$ PSD series. The PSD was then integrated into four classical EEG frequency bands: $\delta[1 - 4)Hz$, $\theta[4 - 8)Hz$, $\alpha[8 - 12)Hz$, $\beta[12 - 32)Hz$, and $\gamma[32 - 45)Hz$. The time-resolved PSD of the HRV series was analogously estimated with a $2Hz$ sampling rate, using a smooth pseudo-Wigner-Ville distribution integrated from $0.04\ Hz$ to $0.15\ Hz$ (LF band) to estimate sympathovagal activity, and from $0.15\ Hz$ to $0.4\ Hz$ (HF band) to estimate vagal activity.

D. BRAIN-HEART INTERPLAY ESTIMATION

BHI quantification was performed using the SDG model presented in a previous study [40]. In this approach, the EEG series refer to a multi-oscillator [61] model whose amplitudes are generated by a first-order exogenous autoregressive (ARX) model, with the exogenous term denoting information transfer from the heart to the brain. In contrast, the RR series are modelled by extending an integral and pulse frequency modulation (IPFM) model proposed previously [62], where the control function of sympathetic and vagal activity quantifies information transfer from the brain to the heart.

In summary, for each combination of EEG bands and HRV frequency components, a dynamic directional BHI series was computed. The main idea behind the conceptualization of this model is that the electrophysiological signals of the two systems are not independent of each other, and the functional coupling terminology attempts to formalize these interactions. Thus, a positive value of $C_{\alpha \rightarrow HF}(t_n)$ indicates that the EEG band α at time t_n has a positive effect (i.e., it leads to a linearly proportional increase) on the PSD from the HRV series in the HF range. This is quantified through the inverse model formulation, which estimates the control function term in the IPFM model related to heartbeat dynamics (i.e., brain-to-heart interplay) and the exogenous term of the ARX model associated with EEG dynamics (i.e., heart-to-brain interplay). The inverse model formulation and derivation of the entire BHI biomarker suite are extensively described in previous studies [10],

TABLE 1. BHI indices extracted through the model.

Index	From	Band	To	Band
$C_{Brain_j \rightarrow Heart_{B_C}}$	Brain	$\delta, \theta, \alpha, \beta, \gamma$	Heart	LF, HF
$C_{Heart_{B_C} \rightarrow Brain_j}$	Heart	LF, HF	Brain	$\delta, \theta, \alpha, \beta, \gamma$

[12], [40], and an easy-to-use MATLAB implementation is freely available [63]. The computational model runs over the entire experimental window and takes the PSD extracted as described in Section II-C as input. At each time instant that the PSD is sampled, the model provides a corresponding time-varying BHI estimation that is sampled coherently with the PSD sampling. This approach ensures that the BHI estimation is accurately synchronized with the physiological signals being analyzed. The directional BHI indices listed in Table 1 were calculated for further consideration.

E. DERIVATION OF COMPLEXITY MAPPING FOR BRAIN-HEART INTERPLAY SERIES

As mentioned previously, the complexity of the BHI time–resolved series $u(i) : 1 \leq i \leq N$ calculated using the SDG model was quantified using the FuzzyEn algorithm [35]. To achieve this, a specific embedding dimension m must be used to reconstruct the system phase space, and the distance d_{ij}^m between two vectors in such a phase space is formulated as follows:

$$d_{ij}^m = \max_{k \in (0, m-1)} \left\{ |u(i + k) - \mathbb{E}\,[u(i)] - (u(j + k) - \mathbb{E}\,[u(j)])| \right\}$$

(1)

where $(i, j = 1 : N - m, j \neq i)$, and $\mathbb{E}$ is the expectation operator. The fuzzy membership function $\mu(d_{ij}^m, n, r)$ was used to define the similarity degree D_{ij}^m, as described in Eq. 2:

$$D_{ij}^m = \mu(d_{ij}^m, n, r) = exp\left(\frac{-(d_{ij}^m)^n}{r}\right)$$

(2)

where n and r are the gradient of the boundary and the width of the exponential function, respectively. At this point, FuzzyEn of an N-point time series can be formulated as follows:

$$FuzzyEn(m, n, r, N) = \lim_{N \rightarrow \infty} [\ln \phi^m(n, r) - \ln \phi^{m+1}(n, r)]$$

(3)

where $\phi^m(n, r)$ is the function

$$\phi^m(n, r) = \frac{1}{N - m} \sum_{i=1}^{N-m} \left[\frac{1}{N - m - 1} \sum_{j=1, j \neq i}^{N-m} D_{ij}^m \right]$$

(4)

The parameter r was set to $r = \rho \cdot SD$, and n was set to 2, in accordance with previous studies [35], [64], where ρ is the tolerance set to 0.2 and SD is defined as the series standard deviation. The pseudo-optimal embedding dimension $m = 3$ is calculated by maximising the probability that the estimate is valid [65]. This work is inspired by our preliminary study [66].

F. STATISTICAL ANALYSIS

For each experimental dataset, FuzzyEn was calculated separately, thereby obtaining a single estimate for each subject and experimental condition. Prior to the complexity quantification through the FuzzyEn algorithm, we statistically assess whether a BHI time series showed nonlinear and complex dynamics by testing two null hypotheses. The first test hypothesized linearity using the nonlinearity test proposed by Barnett and Wolff [67], which uses the third-order moment and bispectrum of the time series, as well as the amplitude-adjusted Fourier transform algorithm to extract surrogate time series [68]. The second test hypothesized chaotic dynamics by testing for a positive Lyapunov exponent using the Jacobian method described by Ellner et al. [69], as implemented by Bensaida [70]. Of note, physiological noise underlying BHI dynamics may contribute to a positive Lyapunov exponent. Only time series that were verified as both nonlinear and chaotic underwent the FuzzyEn implementation. Approximately 99% of the experimental time series were associated with a nonlinear dynamical system and with a positive Lyapunov exponent, and less than 1% of the series were discarded.

Non-parametric statistical analysis for repeated measures was implemented to investigate the differences in BHI complexity between the experimental conditions. The Friedman test was used as a group-wise statistical test with CPT data comparing resting state, cold pressor test, and recovery phase together. Pairwise comparisons were implemented using a non-parametric Wilcoxon test for paired samples on MA data, comparing resting phase to mental calculation, and on CPT data, comparing R vs CPT, R vs recovery, and CPT vs recovery.

We generally set the statistical significance at $\alpha = 0.05$. As the pairwise comparisons on CPT data were repeated three times, we corrected the statistical threshold by applying Bonferroni correction, having $\alpha^1 = \alpha/3 = 0.01667$. All statistical comparisons were performed on FuzzyEn estimates for each EEG channel. To account for multiple comparisons on the channel dimension, we performed a p–value correction using cluster–mass permutation correction, while also assessing the physiological plausibility of the results [71].

Finally, we compared the normalized FuzzyEn values (task condition relative to rest state) between the BC and GC groups using the non-parametric Mann-Whitney test for independent samples. This aimed to explore potential differences in BHI complexity based on the difficulty or performance of the calculation task within the MA dataset.

III. EXPERIMENTAL RESULTS

A. MENTAL ARITHMETICS TASK

The estimation of FuzzyEn on the BHI series gathered from the MA dataset led to different topographical distributions for the combinations of the four EEG and two HRV frequency bands considered. Median across subjects topographies are reported in Figure 1 and 2 of the Supplementary material, related to resting state and MA task phase respectively. The non-parametric statistical comparison of paired samples in the two experimental phases (i.e. resting state and mental arithmetic task) yielded the results presented in Figure 1.a.

The two phases did not significantly differ in terms of BHI estimation in the top–down direction, going from the brain to the heart, or in the opposite direction, considering the HRV–HF frequency band. Significant differences were found in the $BHI_{LF \rightarrow brain}$ complexity estimates, particularly considering the θ and α bands, in the left dorso-parietal and right frontal region for the θ band, and the left temporal and bilateral frontal area for the α band.

Going more deeply into the analysis, the BHI indexes calculated from the two experimental groups split by looking at their arithmetic performances were compared, and the results are presented in Figure 1.b. Specifically, the BHI complexity net variations (for all combinations of frequency bands and scalp locations) given by the experimental elicitation were extracted for each subject (($FuzzyEn(BHI_{MA}) - FuzzyEn(BHI_R))/FuzzyEn(BHI_R)$) to isolate the effect of mental arithmetic. Interestingly, significant differences were found in the top–down direction, particularly involving the HRV–HF frequency bands and all the EEG–derived bands, except for the θ band. Specifically, the $BHI_{\delta \rightarrow HF}$ complexity is different in the central–anterior and left fronto-temporal scalp areas, whereas $BHI_{\alpha \rightarrow HF}$ complexity differences highlight a central scalp region, and almost the same central area with the addition of a left frontal electrode is also highlighted by the statistical analysis of the $BHI_{\beta \rightarrow HF}$ complexity. Notably, these significant differences arise from higher $BHI_{brain \rightarrow HF}$ complexity estimations in the GC group or alternatively lower estimations in the BC group. No further difference, were detected in the bottom–up BHI direction.

B. COLD PRESSOR TEST

The estimation of FuzzyEn on the BHI series gathered from the CPT dataset led to different topographical distributions for the combination of the five EEG and two HRV frequency bands considered. Median across subjects topographies are reported in Figure 3, 4, and 5 of the Supplementary material, related to resting state, CPT, and recovery phase respectively. A non-parametric statistical analysis comparing the experimental conditions (i.e. resting state, CPT, and recovery phase) provided the results presented in Figure 2.

Figure 2.a reports the group–wise statistical comparisons for paired samples performed using the non-parametric Friedman test. The experimental phases do not differ in the complexity of BHI when the vagal HF frequency band is involved, both in the bottom–up and top–down directions, exception given for a right frontal region in the $BHI_{HF \rightarrow \gamma}$ interplay. In contrast, several significant differences are highlighted considering the sympathovagal HRV-LF frequency band. Specifically, in the bottom-up direction $BHI_{LF \rightarrow brain}$ both the δ, θ and α band are diffusely significant. More in detail, all the scalp except for an occipital region is
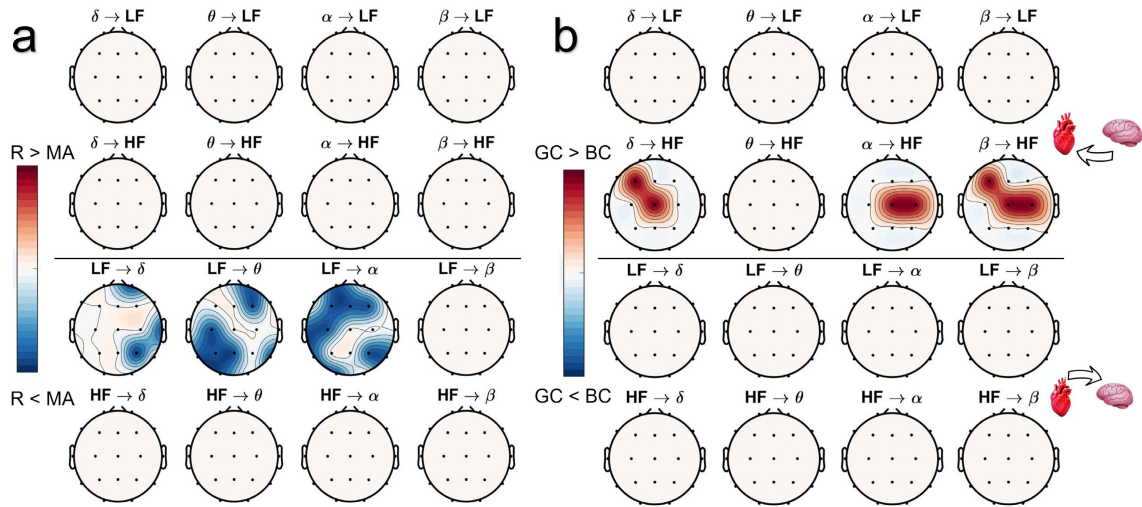
FIGURE 1. Topographical representation of the statistical analysis performed on the MA dataset. The white regions indicate non-significant comparisons, while the red and blue areas show significant differences in which the first or second group had higher values, respectively. Panel a) shows the results of the non-parametric Wilcoxon test for paired samples, which compared the median FuzzyEn of BHI extracted during the resting state (R) and mental arithmetic task (MA). Panel b) shows the results of the non-parametric Mann-Whitney test for independent samples, which compared the normalised difference of the median FuzzyEn of BHI series extracted from the good counter group (GC) and the bad counter group (BC). The normalised difference was calculated as (MA - R)/R.

found significant in the $BHI_{LF \to \alpha}$ complexity analysis, whereas the left temporal and frontal are, as well as the right temporal and dorso parietal are significant considering the $BHI_{LF \to \theta}$ complexity analysis. Intriguingly, statistically significant differences were detected from the analysis of $BHI_{brain \to LF}$ complexity considering the right hemisphere in the EEG-α band, and a left centro-temporal region in the EEG-θ band.

The post-hoc comparison results are shown in Figure 2.b (R *VS* CP) in Figure 2.c (CP *VS* rec), and Figure 2.d (R *VS* rec). The significant differences found in the group–wise comparisons can be ascribed to a higher level of complexity during the initial resting state considering the top-down BHI direction. Indeed, both figures 2.a, and 2.c report significantly higher BHI complexity during the resting state than during both the CP (only the EEG-α band) and recovery phases (in all frequency bands except for the γ band). Thus, the strong sympathovagal elicitation provoked by CPT entails a significant decrease in terms of BHI complexity, which is quite diffuse across the scalp and the EEG spectrum, but limited to the HRV–LF frequency band.

In addition, increasing BHI complexity during CPT phase should be the reason for the significant comparisons highlighted in figures 2.a, 2.b and 2.c in bottom–up $BHI_{LF \to brain}$ statistics. The blue areas are reported in Fig. 2.b, which shows differences between the resting phase and CP, reflecting lower values during rest than in CP, particularly in the $BHI_{LF \to \theta}$ and $BHI_{LF \to alpha}$ complexity, whereas the red regions are reported in fig. 2.c, reflecting higher values during CP with respect to recovery, in all $BHI_{LF \to brain}$ band complexities, and diffuse across the scalp. Eventually, the $BHI_{HF \to \gamma}$ significant differences highlighted in Fig. 2.a, looking at Fig. 2.d seem

to be associated to a decrease in complexity from the resting state to the recovery phase.

IV. DISCUSSION AND CONCLUSION

The high level of complexity in EEG and HRV time series has been extensively studied under several conditions, and the central and autonomic nervous systems are widely known to have a physiological interplay whose dynamics are affected by, and reasonably affect, patho-physiological changes; nevertheless, complexity at the BHI level has not yet been properly assessed. To this end, in this study, the complexity modulation of a functional BHI series was investigated using two different datasets with diverse experimental environments. Time–resolved functional directional BHI has been estimated with an *ad hoc* model combining EEG and HRV series [40] for both heart–to–brain and brain–to–heart directions and considering multiple frequency bands accounting for cerebral and cardiovascular activity. Complexity in the BHI time series was quantified using the FuzzyEn algorithm owing to its reported robustness to noise and low sensitivity to parameter selection, together with its specificity, being a complexity measure, compared to the more commonly used approximate or sample entropy.

The experimental results confirm that the functional BHI series may be considered as the output of a nonlinear system whose complexity is modulated by physiological changes. Moreover, such complexity modulation seems to occur in both the directions of the phenomenon (i.e. heart–to–brain and brain–to–heart), over non–specific brain regions, and over different EEG and HRV frequency bands.

More specifically, a cognitive workload task such as the repetitive subtractions required in the MA dataset led to
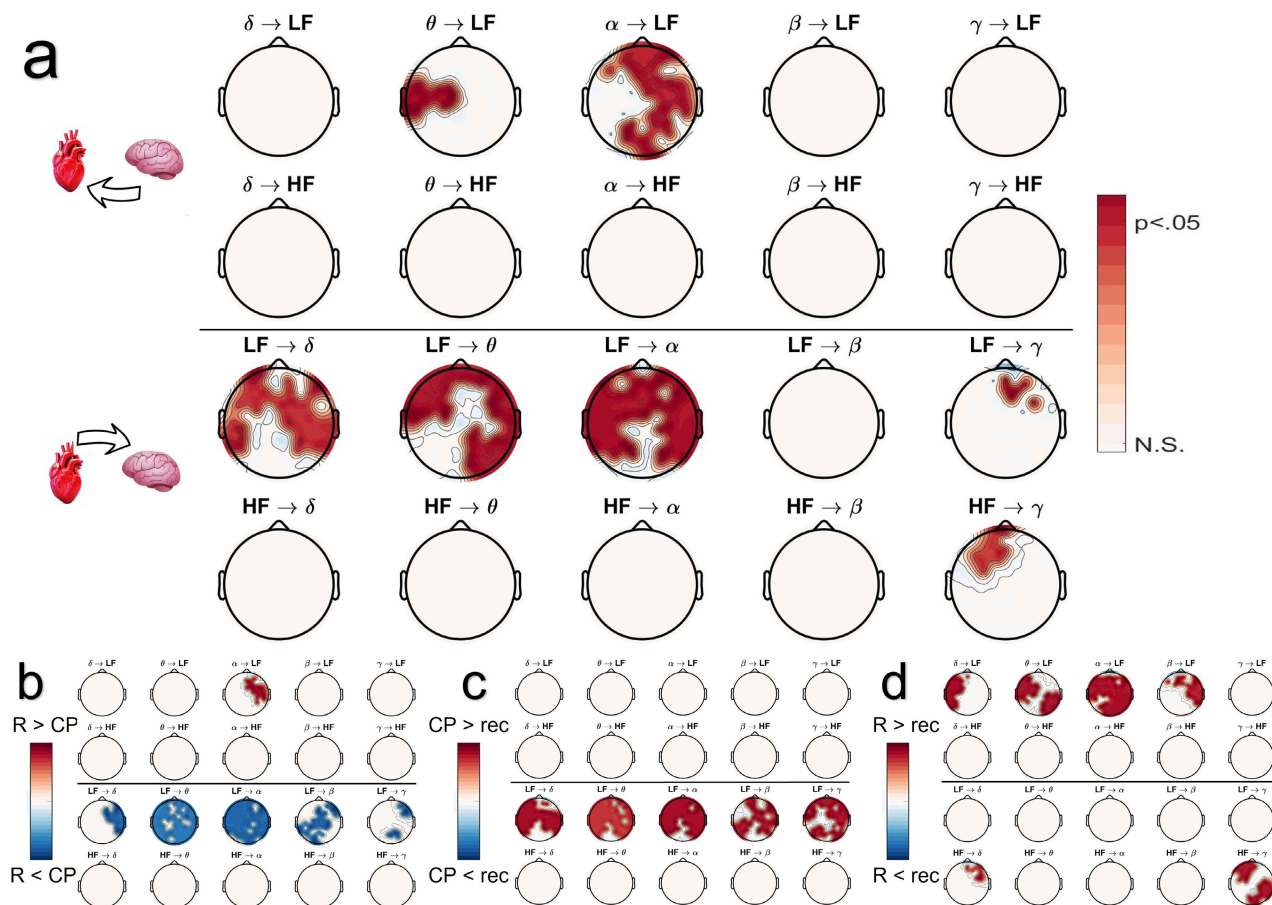
FIGURE 2. Topographical representation of the statistical analysis performed on the CPT dataset. Panel a) shows the results of the non-parametric Friedman test for paired samples, which compared the median FuzzyEn of BHI extracted during resting state (R), cold pressor test (CP), and recovery phase (rec). White regions indicate non-significant comparisons, while red areas represent significant differences. Panels b), c), and d) show the results of the non-parametric Wilcoxon test for paired samples, comparing the median FuzzyEn of BHI during R-vs-CP (b) , CP-VS-rec (c), and R-VS-rec (d). White regions represent non-significant comparisons, red areas indicate significant differences in which the first group had higher values than the second, and blue sections represent the opposite.

a significant increase in BHI complexity in the direction from the heart to the brain, involving the sympathovagal component LF of the cardiovascular activity spectrum and diffuse regions of the scalp particularly considering the EEG–θ and α oscillations (see Fig. 1). Intriguingly, statistically significant regions were detected by comparing the BHI complexity of the two experimental groups, individuated by [54] and differentiated according to their arithmetic performance (the number of calculations reached in the same amount of time). Specifically, the GC group showed higher BHI complexity in the direction from the brain to the heart, involving EEG– δ (in a central region), α (in right parietal area), and β (in similar scalp locations) frequency bands. This may suggest that the cognitive workload such as the MA diffusely affect ascending BHI complexity, and different amounts of stress are induced by the same task in two separate groups of people. Indeed, previous studies have already analysed the MA dataset, and there is a general consensus regarding the low levels of stress in the GC group (i.e., the one with better arithmetic performance) and the high stress

levels in the BC group [72], [73], [74], [75], [76]. Keeping this in mind, future studies should aim to further evaluate whether the stress level modulates BHI complexity more than the cognitive load *per se*.

The analysis of the CPT dataset, which has already been extensively employed in studies of absolute changes in functional BHI [16], [30], [48], yielded significant insights into BHI dynamics. Previous studies have already shown that BHI intensity is strongly affected by CPT elicitation [16], [40], [48], cerebral and cardiovascular multifractal dynamics are coupled [30], and BHI changes are not strictly limited to the CPT phase, but the return to homeostatic equilibrium persists during recovery [22], [48]. Now we also know that CPT–elicited BHI changes extend to the complexity domain in a very peculiar way, particularly in relation to the sympathovagal HRV–LF frequency range. Significant group-wise variations are detected in the brain–to–LF direction, and the bottom sub-panels in Fig. 2 indicate that these variations are entirely imputable to a significant decrease in BHI complexity after the stimulation onset (CPT beginning),

with respect to the resting state, that persists even during recovery.

Conversely, in the opposite direction, a temporary significant increase in complexity may occur during CPT, which then returns to normal during the recovery phase. These modulations primarily appear in both hemispheres (based on group-wise comparisons) within a frequency band ranging from 1 to 12Hz (encompassing δ, θ, and α bands), and exhibit a higher level of detail in pair-wise comparisons (i.e., rest *VS* CPT and CPT *VS* recovery). Indeed, in one study [48], a consistent and bidirectional significant BHI intensity variation was found between the same EEG frequency bands and the sympathetic activity, as in [16], where unidirectional brain–to–heart information transfer was investigated. Notably, a previous study [48] also reported significant variations in the interplay between EEG bands and vagal-specific activity from the resting state to CPT and from CPT to recovery. This does not disagree with the results reported here, since the HRV–LF frequency range is not a specific biomarker, being related to both sympathetic and vagal activity. Taken together, the results of the present study and those in the related literature suggest that the variations in BHI intensity found to be associated with the HRV–LF band extend to the nonlinear and complex dynamics, whereas those associated with the HRV–HF band do not.

The fact that the interplay between cerebral and cardiovascular dynamics shows a complex behaviour was a clear finding in the present study, supported by both the knowledge that the two systems *per se* have complex behaviours and that the underlying interplay involves multiple structures and can be associated with multiple feedback mechanisms occurring (but not limited to) at the hormonal, mechanical, and electrical levels. This observation is further supported by the fact that functional BHI encompasses the multifractal domain [30], thereby introducing an additional level of complexity. Nevertheless, BHI complexity has not been investigated to date, and the authors believe that its modulation should be further addressed in studies focused on the several patho-physiological conditions associated to BHI dynamic changes, including mental or mood disorders.

The limitations of this study are mainly related to the limited parameter space investigated; indeed, an exhaustive exploration of such a space would provide a better understanding of the phenomenon, and parameter optimisation associated with the specific patho-physiological conditions under study should be of interest.

The translational medicine aspects of quantitatively assessing functional brain-heart interplay through EEG and ECG signals can contribute to the diagnosis and treatment of various disorders. For instance, BHI-related biomarkers has been used to study the effects of neurological conditions like epilepsy, Alzheimer's disease, and Parkinson's disease on cardiac function [77], [78]. Similarly, it has been employed to investigate the impact of cardiovascular diseases, such as myocardial infarction and arrhythmias, on brain activity [79]. Furthermore, it has shown potential in predicting treatment

outcomes and monitoring the effectiveness of therapeutic interventions [80].

In conclusion, this study showed that the BHI dynamics have a complex behaviour which changes across the scalp, spectrum, and experimental case, providing meaningful insights into brain–heart neurophysiology and enriching the set of biomarkers that may be used for dynamic characterisation of the system as a whole.

REFERENCES

[1] V. Catrambone and G. Valenza, *Functional Brain-Heart Interplay*. Switzerland: Springer, 2021.

[2] R. Pernice, L. Faes, M. Feucht, F. Benninger, S. Mangione, and K. Schiecke, "Pairwise and higher-order measures of brain-heart interactions in children with temporal lobe epilepsy," *J. Neural Eng.*, vol. 19, no. 4, Aug. 2022, Art. no. 045002.

[3] P. Taggart, H. Critchley, and P. D. Lambiase, "Heart-brain interactions in cardiac arrhythmia," *Heart*, vol. 97, no. 9, pp. 698–708, May 2011.

[4] J. Thome et al., "Desynchronization of autonomic response and central autonomic network connectivity in posttraumatic stress disorder," *Hum. Brain Mapping*, vol. 38, no. 1, pp. 27–40, Jan. 2017.

[5] E. E. Benarroch, "The central autonomic network: Functional organization, dysfunction, and perspective," *Mayo Clinic Proc.*, vol. 68, no. 10, pp. 988–1001, Oct. 1993.

[6] G. Valenza et al., "The central autonomic network at rest: Uncovering functional MRI correlates of time-varying autonomic outflow," *NeuroImage*, vol. 197, pp. 383–390, Aug. 2019.

[7] G. Valenza, L. Passamonti, A. Duggento, N. Toschi, and R. Barbieri, "Uncovering complex central autonomic networks at rest: A functional magnetic resonance imaging study on complex cardiovascular oscillations," *J. Roy. Soc. Interface*, vol. 17, no. 164, Mar. 2020, Art. no. 20190878.

[8] L. Quadt, H. Critchley, and Y. Nagai, "Cognition, emotion, and the central autonomic network," *Autonomic Neurosci.*, vol. 238, Mar. 2022, Art. no. 102948.

[9] S. Govoni, P. Politi, and E. Vanoli, Eds., *Brain and Heart Dynamics*. Cham, Switzerland: Springer, 2020.

[10] V. Catrambone, S. M. Benvenuti, C. Gentili, and G. Valenza, "Intensification of functional neural control on heartbeat dynamics in subclinical depression," *Transl. Psychiatry*, vol. 11, no. 1, pp. 1–10, Apr. 2021.

[11] E. E. Benarroch, "Physiology and pathophysiology of the autonomic nervous system," *Continuum, Lifelong Learn. Neurol.*, vol. 26, no. 1, pp. 12–24, Feb. 2020.

[12] D. Candia-Rivera, V. Catrambone, J. F. Thayer, C. Gentili, and G. Valenza, "Cardiac sympathetic-vagal activity initiates a functional brain–body response to emotional arousal," *Proc. Nat. Acad. Sci. USA*, vol. 119, no. 21, May 2022.

[13] A. Silvani, G. Calandra-Buonaura, R. A. L. Dampney, and P. Cortelli, "Brain–heart interactions: Physiology and clinical implications," *Phil. Trans. Roy. Soc. A, Math., Phys. Eng. Sci.*, vol. 374, no. 2067, May 2016, Art. no. 20150181.

[14] X. Yu, C. Zhang, L. Su, J. Zhang, and N. Rao, "Estimation of the cortico-cortical and brain-heart functional coupling with directed transfer function and corrected conditional entropy," *Biomed. Signal Process. Control*, vol. 43, pp. 110–116, May 2018.

[15] R. Jerath and V. A. Barnes, "Augmentation of mind-body therapy and role of deep slow breathing," *J. Complementary Integrative Med.*, vol. 6, no. 1, Jan. 2009.

[16] V. Catrambone, A. Talebi, R. Barbieri, and G. Valenza, "Time-resolved brain-to-heart probabilistic information transfer estimation using inhomogeneous point-process models," *IEEE Trans. Biomed. Eng.*, vol. 68, no. 11, pp. 3366–3374, Nov. 2021.

[17] G. Calandra-Buonaura et al., "Physiologic autonomic arousal heralds motor manifestations of seizures in nocturnal frontal lobe epilepsy: Implications for pathophysiology," *Sleep Med.*, vol. 13, no. 3, pp. 252–262, Mar. 2012.

[18] S. Schulz, N. Tupaika, S. Berger, J. Haueisen, K.-J. Bär, and A. Voss, "Cardiovascular coupling analysis with high-resolution joint symbolic dynamics in patients suffering from acute schizophrenia," *Physiological Meas.*, vol. 34, no. 8, pp. 883–901, Aug. 2013.

[19] E. Al et al., "Heart–brain interactions shape somatosensory perception and evoked potentials," *Proc. Nat. Acad. Sci. USA*, vol. 117, no. 19, pp. 10575–10584, 2020.

[20] K. Schiecke, A. Schumann, F. Benninger, M. Feucht, K.-J. Baer, and P. Schlattmann, "Brain–heart interactions considering complex physiological data: Processing schemes for time-variant, frequency-dependent, topographical and statistical examination of directed interactions by convergent cross mapping," *Physiological Meas.*, vol. 40, no. 11, Nov. 2019, Art. no. 114001.

[21] A. Greco, L. Faes, V. Catrambone, R. Barbieri, E. P. Scilingo, and G. Valenza, "Lateralization of directional brain-heart information transfer during visual emotional elicitation," *Amer. J. Physiol.-Regulatory, Integrative Comparative Physiol.*, vol. 317, no. 1, pp. R25–R38, Jul. 2019.

[22] V. Catrambone and G. Valenza, "Nervous–system–wise functional estimation of directed brain–heart interplay through microstate occurrences," *IEEE Trans. Biomed. Eng.*, early access, Jan. 30, 2023, doi: 10.1109/TBME.2023.3240593.

[23] L. Faes, D. Marinazzo, F. Jurysta, and G. Nollo, "Linear and non-linear brain–heart and brain–brain interactions during sleep," *Physiological Meas.*, vol. 36, no. 4, pp. 683–698, Apr. 2015.

[24] L. Faes, D. Kugiumtzis, G. Nollo, F. Jurysta, and D. Marinazzo, "Estimating the decomposition of predictive information in multivariate systems," *Phys. Rev. E, Stat. Phys. Plasmas Fluids Relat. Interdiscip. Top.*, vol. 91, no. 3, Mar. 2015, Art. no. 032904.

[25] K. Sunagawa, T. Kawada, and T. Nakahara, "Dynamic nonlinear vago-sympathetic interaction in regulating heart rate," *Heart Vessels*, vol. 13, no. 4, pp. 157–174, Jul. 1998.

[26] U. R. Acharya, K. P. Joseph, N. Kannathal, C. M. Lim, and J. S. Suri, "Heart rate variability: A review," *Med. Biol. Eng. Comput.*, vol. 44, no. 12, pp. 1031–1051, Dec. 2006.

[27] C. J. Stam, "Nonlinear dynamical analysis of EEG and MEG: Review of an emerging field," *Clin. Neurophysiol.*, vol. 116, no. 10, pp. 2266–2301, Oct. 2005.

[28] A. Scarciglia, V. Catrambone, C. Bonanno, and G. Valenza, "A multiscale partition-based Kolmogorov–Sinai entropy for the complexity assessment of heartbeat dynamics," *Bioengineering*, vol. 9, no. 2, p. 80, Feb. 2022.

[29] X.-S. Zhang, R. J. Roy, and E. W. Jensen, "EEG complexity as a measure of depth of anesthesia for patients," *IEEE Trans. Biomed. Eng.*, vol. 48, no. 12, pp. 1424–1433, 2001.

[30] V. Catrambone, R. Barbieri, H. Wendt, P. Abry, and G. Valenza, "Functional brain–heart interplay extends to the multifractal domain," *Phil. Trans. Roy. Soc. A, Math., Phys. Eng. Sci.*, vol. 379, no. 2212, Dec. 2021, Art. no. 20200260.

[31] M. Valente et al., "Univariate and multivariate conditional entropy measures for the characterization of short-term cardiovascular complexity under physiological stress," *Physiological Meas.*, vol. 39, no. 1, Jan. 2018, Art. no. 014002.

[32] L. Faes and A. Porta, "Conditional entropy-based evaluation of information dynamics in physiological systems," in *Directed Information Measures in Neuroscience*. Berlin, Germany: Springer, 2014, pp. 61–86.

[33] S. M. Pincus, "Approximate entropy as a measure of system complexity.," *Proc. Nat. Acad. Sci. USA*, vol. 88, no. 6, pp. 2297–2301, Mar. 1991.

[34] J. S. Richman and J. R. Moorman, "Physiological time-series analysis using approximate entropy and sample entropy," *Amer. J. Physiol.-Heart Circulatory Physiol.*, vol. 278, no. 6, pp. H2039–H2049, Jun. 2000.

[35] W. Chen, Z. Wang, H. Xie, and W. Yu, "Characterization of surface EMG signal based on fuzzy entropy," *IEEE Trans. Neural Syst. Rehabil. Eng.*, vol. 15, no. 2, pp. 266–272, Jun. 2007.

[36] C. C. Mayer, M. Bachler, M. Hörtenhuber, C. Stocker, A. Holzinger, and S. Wassertheurer, "Selection of entropy-measure parameters for knowledge discovery in heart rate variability data," *BMC Bioinf.*, vol. 15, no. S6, p. S2, May 2014.

[37] W. Chen, J. Zhuang, W. Yu, and Z. Wang, "Measuring complexity using FuzzyEn, ApEn, and SampEn," *Med. Eng. Phys.*, vol. 31, no. 1, pp. 61–68, Jan. 2009.

[38] S. Simons, P. Espino, and D. Abásolo, "Fuzzy entropy analysis of the electroencephalogram in patients with Alzheimer's disease: Is the method superior to sample entropy?" *Entropy*, vol. 20, no. 1, p. 21, Jan. 2018.

[39] C. Liu et al., "Analysis of heart rate variability using fuzzy measure entropy," *Comput. Biol. Med.*, vol. 43, no. 2, pp. 100–108, Feb. 2013.

[40] V. Catrambone, A. Greco, N. Vanello, E. P. Scilingo, and G. Valenza, "Time-resolved directional brain–heart interplay measurement through synthetic data generation models," *Ann. Biomed. Eng.*, vol. 47, no. 6, pp. 1479–1489, Jun. 2019.

[41] A. Zygmunt and J. Stanczyk, "Methods of evaluation of autonomic nervous system function," *Arch. Med. Sci.*, vol. 1, no. 1, pp. 11–18, 2010.

[42] T. Inouye, K. Shinosaki, A. Iyama, and Y. Matsumoto, "Localization of activated areas and directional EEG patterns during mental arithmetic," *Electroencephalogr. Clin. Neurophysiol.*, vol. 86, no. 4, pp. 224–230, Apr. 1993.

[43] Q. Wang and O. Sourina, "Real-time mental arithmetic task recognition from EEG signals," *IEEE Trans. Neural Syst. Rehabil. Eng.*, vol. 21, no. 2, pp. 225–232, Mar. 2013.

[44] L. Bernardi et al., "Effects of controlled breathing, mental activity and mental stress with or without verbalization on heart rate variability," *J. Amer. College Cardiol.*, vol. 35, no. 6, pp. 1462–1469, May 2000.

[45] M. A. Gray et al., "A cortical potential reflecting cardiac function," *Proc. Nat. Acad. Sci. USA*, vol. 104, no. 16, pp. 6818–6823, Apr. 2007.

[46] D. Candia-Rivera, K. Norouzi, T. Z. Ramsøy, and G. Valenza, "Dynamic fluctuations in ascending heart-to-brain communication under mental stress," *Amer. J. Physiol.-Regulatory, Integrative Comparative Physiol.*, vol. 324, no. 4, pp. R513–R525, Apr. 2023.

[47] H. Yuan, T. Liu, R. Szarkowski, C. Rios, J. Ashe, and B. He, "Negative covariation between task-related responses in alpha/beta-band activity and BOLD in human sensorimotor cortex: An EEG and fMRI study of motor imagery and movements," *NeuroImage*, vol. 49, no. 3, pp. 2596–2606, Feb. 2010.

[48] D. Candia-Rivera, V. Catrambone, R. Barbieri, and G. Valenza, "Functional assessment of bidirectional cortical and peripheral neural control on heartbeat dynamics: A brain-heart study on thermal stress," *NeuroImage*, vol. 251, May 2022, Art. no. 119023.

[49] W. Lovallo, "The cold pressor test and autonomic function: A review and integration," *Psychophysiology*, vol. 12, no. 3, pp. 268–282, May 1975.

[50] J. Cui, T. E. Wilson, and C. G. Crandall, "Baroreflex modulation of muscle sympathetic nerve activity during cold pressor test in humans," *Amer. J. Physiol.-Heart Circulatory Physiol.*, vol. 282, no. 5, pp. H1717–H1723, May 2002.

[51] S. Ferracuti, S. Seri, D. Mattia, and G. Cruccu, "Quantitative EEG modifications during the cold water pressor test: Hemispheric and hand differences," *Int. J. Psychophysiol.*, vol. 17, no. 3, pp. 261–268, Aug. 1994.

[52] D. U. Silverthorn and J. Michael, "Cold stress and the cold pressor test," *Adv. Physiol. Educ.*, vol. 37, no. 1, pp. 93–96, Mar. 2013.

[53] P. F. Chang, L. Arendt-Nielsen, and A. C. N. Chen, "Dynamic changes and spatial correlation of EEG activities during cold pressor test in man," *Brain Res. Bull.*, vol. 57, no. 5, pp. 667–675, Mar. 2002.

[54] I. Zyma et al., "Electroencephalograms during mental arithmetic task performance," *Data*, vol. 4, no. 1, p. 14, 2019.

[55] A. L. Goldberger et al., "PhysioBank, PhysioToolkit, and PhysioNet: Components of a new research resource for complex physiologic signals," *Circulation*, vol. 101, no. 23, pp. e215–e220, Jun. 2000.

[56] D. Candia-Rivera, V. Catrambone, and G. Valenza, "The role of electroencephalography electrical reference in the assessment of functional brain–heart interplay: From methodology to user guidelines," *J. Neurosci. Methods*, vol. 360, Aug. 2021, Art. no. 109269.

[57] J. Pan and W. J. Tompkins, "A real-time QRS detection algorithm," *IEEE Trans. Biomed. Eng.*, vol. BME-32, no. 3, pp. 230–236, Mar. 1985.

[58] M. P. Tarvainen, J.-P. Niskanen, J. A. Lipponen, P. O. Ranta-Aho, and P. A. Karjalainen, "Kubios HRV–heart rate variability analysis software," *Comput. Methods Programs Biomed.*, vol. 113, no. 1, pp. 210–220, 2014.

[59] L. J. Gabard-Durnam, A. S. Mendez Leal, C. L. Wilkinson, and A. R. Levin, "The Harvard automated processing pipeline for electroencephalography (HAPPE): Standardized processing software for developmental and high-artifact data," *Frontiers Neurosci.*, vol. 12, p. 97, Feb. 2018.

[60] A. Delorme and S. Makeig, "EEGLAB: An open source toolbox for analysis of single-trial EEG dynamics including independent component analysis," *J. Neurosci. Methods*, vol. 134, no. 1, pp. 9–21, Mar. 2004.

[61] H. Al-Nashash, Y. Al-Assaf, J. Paul, and N. Thakor, "EEG signal modeling using adaptive Markov process amplitude," *IEEE Trans. Biomed. Eng.*, vol. 51, no. 5, pp. 744–751, May 2004.

[62] M. Brennan, M. Palaniswami, and P. Kamen, "Poincaré plot interpretation using a physiological model of HRV based on a network of oscillators," *Amer. J. Physiol.-Heart Circulatory Physiol.*, vol. 283, no. 5, pp. H1873–H1886, Nov. 2002.

[63] V. Catrambone. (2019). *Brain-Heart Interaction Indexes*. [Online]. Available: https://it.mathworks.com/matlabcentral/fileexchange/72704-brain-heart-interaction-indexes

[64] F. Kaffashi, R. Foglyano, C. G. Wilson, and K. A. Loparo, "The effect of time delay on approximate & sample entropy calculations," *Phys. D, Nonlinear Phenomena*, vol. 237, no. 23, pp. 3069–3074, Dec. 2008.

[65] T. L. Carroll and J. M. Byers, "Dimension from covariance matrices," *Chaos, Interdiscipl. J. Nonlinear Sci.*, vol. 27, no. 2, Feb. 2017, Art. no. 023101.

[66] V. Catrambone, E. Patron, C. Gentili, and G. Valenza, "Complexity modulation in functional brain-heart interplay series driven by emotional stimuli: An early study using fuzzy entropy," in *Proc. 44th Annu. Int. Conf. IEEE Eng. Med. Biol. Soc. (EMBC)*, Jul. 2022, pp. 2306–2309.

[67] A. G. Barnett and R. C. Wolff, "A time-domain test for some types of nonlinearity," *IEEE Trans. Signal Process.*, vol. 53, no. 1, pp. 26–33, Jan. 2005.

[68] J. Theiler, S. Eubank, A. Longtin, B. Galdrikian, and J. Doyne Farmer, "Testing for nonlinearity in time series: The method of surrogate data," *Phys. D, Nonlinear Phenomena*, vol. 58, nos. 1–4, pp. 77–94, Sep. 1992.

[69] S. Ellner, A. R. Gallant, D. McCaffrey, and D. Nychka, "Convergence rates and data requirements for jacobian-based estimates of Lyapunov exponents from data," *Phys. Lett. A*, vol. 153, nos. 6–7, pp. 357–363, Mar. 1991.

[70] A. BenSaïda, "A practical test for noisy chaotic dynamics," *SoftwareX*, vols. 3–4, pp. 1–5, Dec. 2015.

[71] K. J. Friston, K. J. Worsley, R. S. J. Frackowiak, J. C. Mazziotta, and A. C. Evans, "Assessing the significance of focal activations using their spatial extent," *Human Brain Mapping*, vol. 1, no. 3, pp. 210–220, 1994.

[72] O. Attallah, "An effective mental stress state detection and evaluation system using minimum number of frontal brain electrodes," *Diagnostics*, vol. 10, no. 5, p. 292, May 2020.

[73] K. Ahammed and M. U. Ahmed, "Quantification of mental stress using complexity analysis of EEG signals," *Biomed. Eng., Appl., Basis Commun.*, vol. 32, no. 2, Apr. 2020, Art. no. 2050011.

[74] K. Kim, N. T. Duc, M. Choi, and B. Lee, "EEG microstate features according to performance on a mental arithmetic task," *Sci. Rep.*, vol. 11, no. 1, pp. 1–14, Jan. 2021.

[75] B. Fatimah, D. Pramanick, and P. Shivashankaran, "Automatic detection of mental arithmetic task and its difficulty level using EEG signals," in *Proc. 11th Int. Conf. Comput., Commun. Netw. Technol. (ICCCNT)*, Jul. 2020, pp. 1–6.

[76] N. Salankar, D. Koundal, and S. M. Qaisar, "Stress classification by multimodal physiological signals using variational mode decomposition and machine learning," *J. Healthcare Eng.*, vol. 2021, pp. 1–12, Aug. 2021.

[77] Y. Sharabi, G. D. Vatine, and A. Ashkenazi, "Parkinson's disease outside the brain: Targeting the autonomic nervous system," *Lancet Neurol.*, vol. 20, no. 10, pp. 868–876, Oct. 2021.

[78] M. Yang, C. Li, Y. Zhang, and J. Ren, "Interrelationship between Alzheimer's disease and cardiac dysfunction: The brain–heart continuum?" *Acta Biochimica et Biophysica Sinica*, vol. 52, no. 1, pp. 1–8, Jan. 2020.

[79] S. Pyner, "The paraventricular nucleus and heart failure," *Exp. Physiol.*, vol. 99, no. 2, pp. 332–339, Feb. 2014.

[80] V. Lionetti et al., "Understanding the heart-brain axis response in COVID-19 patients: A suggestive perspective for therapeutic development," *Pharmacological Res.*, vol. 168, Jun. 2021, Art. no. 105581.

• • •